The National Center for Voice and Speech Online Technical Memo No.3, April 2004, version 1.1

Dynamics of a three-dimensional model of vocal fold abduction/adduction

Eric J. Hunter [1] and Ingo R. Titze [1,2]

[1] National Center for Voice and Speech,
The Denver Center for the Performing Arts, 1245 Champa Street, Denver, CO 80204, USA,

[2] Department of Speech Pathology and Audiology
The University of Iowa, 330-WJSHC, Iowa City, IA 52242, USA

This memo serves as an addition to the paper: E. J. Hunter, I. R. Titze, and F. Alipour, A three-dimensional model of vocal fold adduction/abduction. J.Acoust.Soc.Am. 115 (4):1747-1759, (2004) and to the University of Iowa dissertation E. J. Hunter, Three dimensional biomechanical model of vocal fold posturing, (2001). The contents of the memo provide: (1) an overview of the model with additional detail of the muscle models; (2) the resulting dynamics of the model; and (3) the details of scripts used to model laryngeal muscles which are imbedded into the larger finite element model (the scripts are provided with this memo). The scripts were written in ANSYS Parametric Design Language (APDL), many of which were originally based on FORTRAN code written by Ingo Titze (not provided with this memo). APDL scripts and updates to this memo can be downloaded at http://www.ncvs.org/ncvs/library/tech .

Keywords: vocal posturing, abduction, adduction, finite element modeling, muscle models.

1. Review of the vocal fold posturing model construction

The Hunter abductory/adductory posturing model (targeting a human male larynx, Figure 1.1, with the cricoid cartilage as the reference frame, Figure 1.2) captured two principal features of the laryngeal system: 1) the CAJ, which was designed to preserve its three-dimensional rocking-sliding movement (Selbie et al., 1998); and 2) the vocal fold intrinsic fibers, which included the laryngeal muscles and vocal ligament. The laryngeal muscles incorporated into the model were the four intrinsic muscles attached to the arytenoid: TA, PCA, IA, and LCA (Figure 1.3, orientation taken from Mineck et al., 2000). The two major bellies of the TA were treated as if they were two separate muscles, the thyrovocalis (TAV) and thyromuscularis (TAM) (orientation taken from Cox et al., 1999; see Figure 1.4 for overall composite). The model was dynamic and, thus, included deformation of vocal fold tissues.

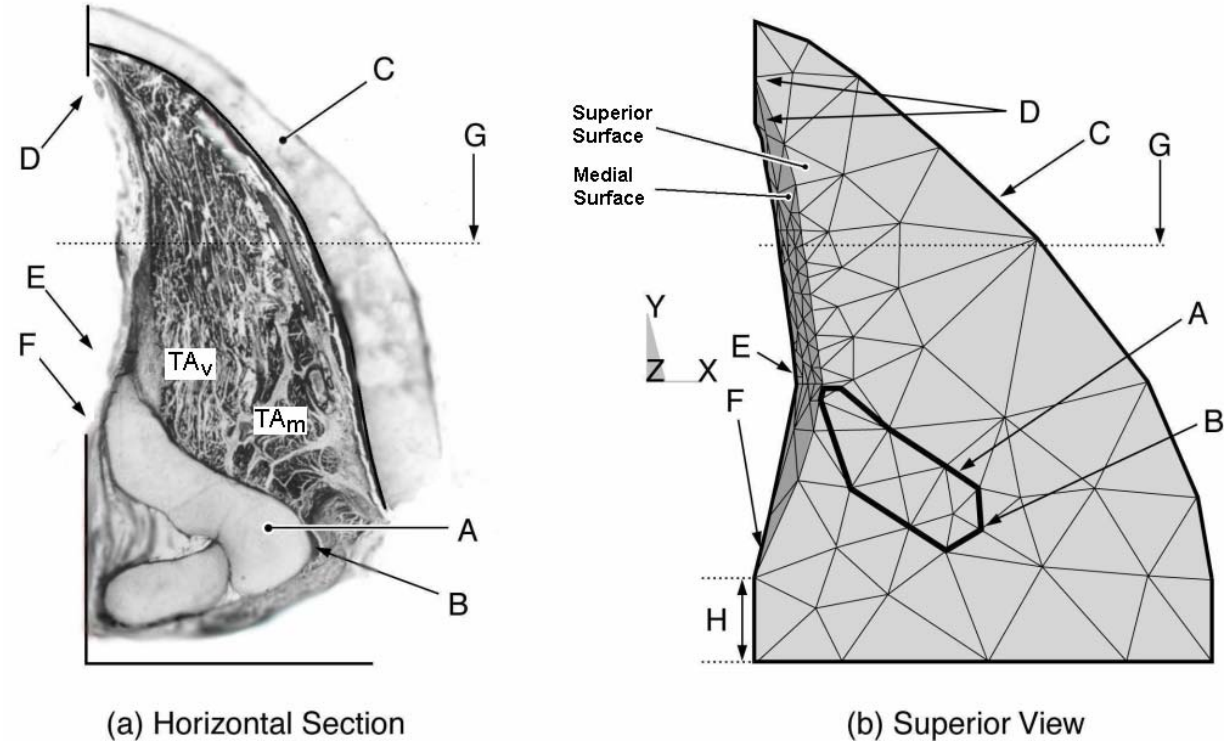

Figure 1.1. The right vocal fold: (a) horizontal slice at the level of the vocal process; and (b) view of model from above. Vocal fold landmarks: A - the arytenoid cartilage, B - muscular process, C - thyroid cartilage, D - anterior commissure, E - vocal process, F - posterior commissure, G - mid-membranous vocal fold line, and H - posterior border.

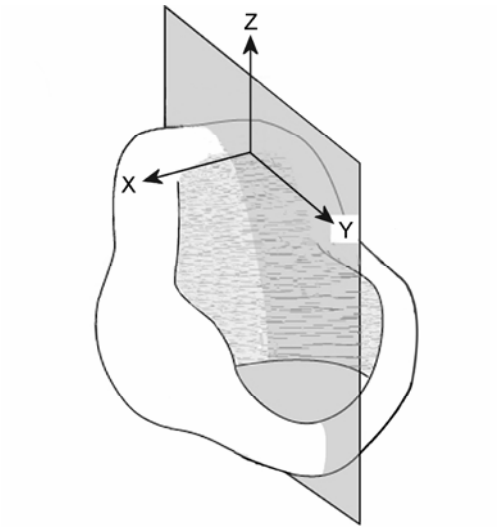

Figure 1.2. Coordinate system from vantage point of cricoid cartilage (after Selbie, et al., 1998).

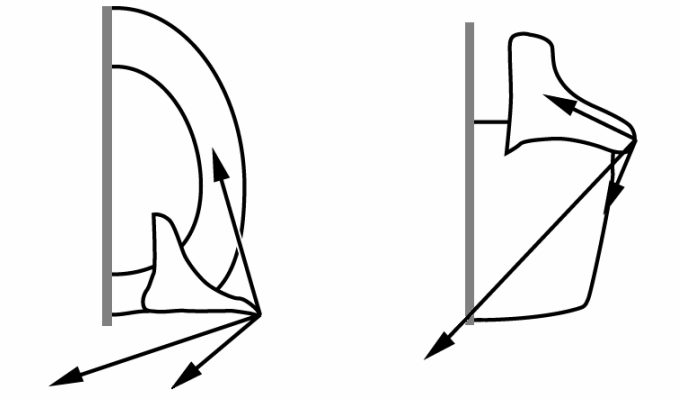

Figure 1.3. Force vectors of the LCA, PCA and IA (after Mineck, Tayama, Chan, and Titze, 2000).

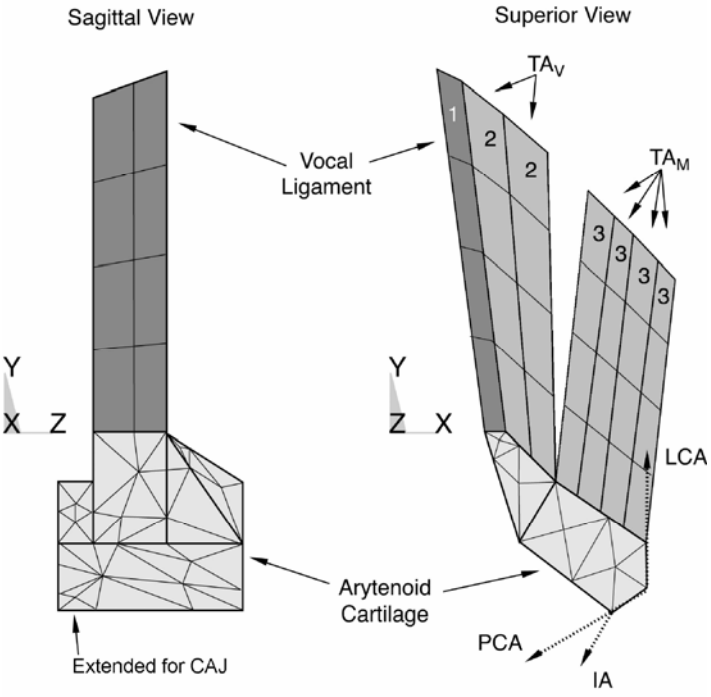

Figure 1.4. Modeled arytenoid cartilage and fiber-gel composite volumes (only outer element faces are shown). Three types of modeled fiber-gels: TAM, TAV, and vocal ligament. Intrinsic adductor and abductor muscles (PCA, LCA, and IA) attached near the muscular process. Dotted vectors in the superior view represent the applied forces (x-y component shown only) of these three muscles.

All vocal fold intrinsic fibers in the posturing model had contractile and/or passive nonlinear stress-strain properties as predicted by a modified Kelvin model (Figure 1.5). From Equations 13-17 in Hunter et al. (2004), the passive characteristics can be predicted (Figure 1.6).

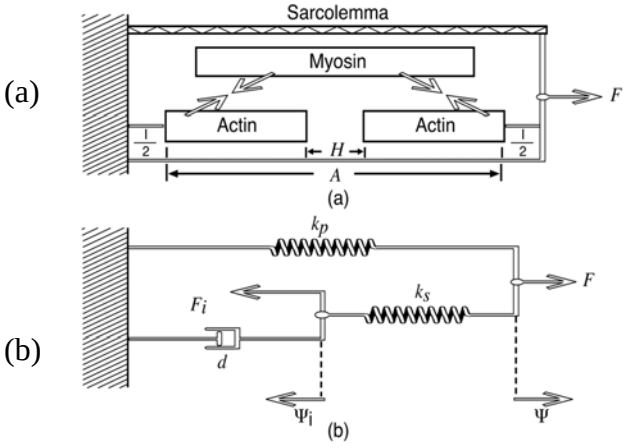

Figure 1.5. (a) One sarcomere length of a muscle fibril, (b) Kelvin model for mechanical response.

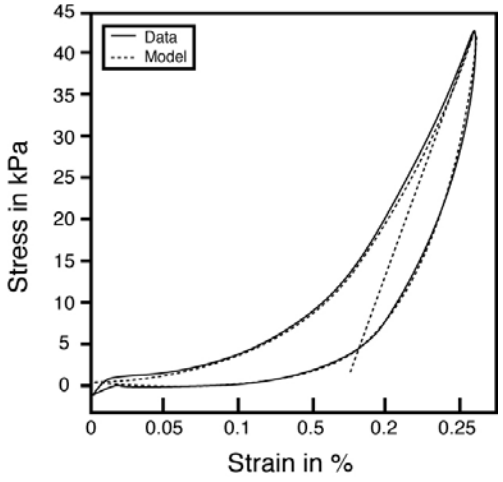

Figure 1.6. Passive stress-strain response for canine thyroarytenoid muscle. Shown are: (1) measured cyclic (1 Hz) elongation data (solid line), (2) Titze fiber model response after being fit to data (dotted line), and (3) piece-wise stress-strain relation with no viscous losses (dashed line) representing gel response.

In a similar fashion, from Equations 18-22, the active or contractile properties of a muscle can be modeled. Figure 1.7a shows a twitch as predicted by the equations, given a single pulse activation at several strains. Figure 1.7b is similar but show a tetanus (longer activation).

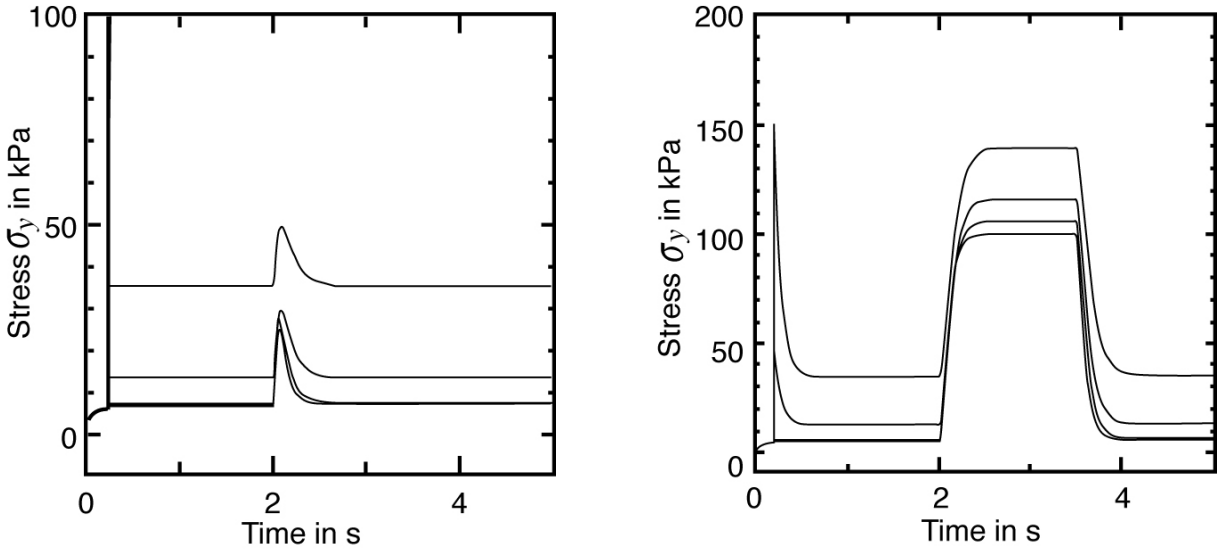

(a) (b)

Figure 1.7. (a) Simulation of a muscle twitch with the muscle model. (b) Tetanus simulation of the muscle model. The family of curves in (a) and (b) corresponds to different values of strain (0%, 10%, 20%, 30%,. 40%).

The fiber characteristics of the muscles and vocal ligament were implemented using a fiber-gel composite made of an isotropic ground substance embedded with uni-dimensional fibers, Figure 1.8.

Hunter et al. (2004) illustrated the fiber-gel construct by modeling an elongation and contraction of a muscle in isolation. Multimedia movies of each can be seen.

low resolution (small file)
isolated contract contraction:
http://www.ncvs.org/ncvs/library/tech/note3/low/musc3d_contract.gif
elongate contract contraction:
http://www.ncvs.org/ncvs/library/tech/note3/low/musc3d_elong.gif

high resolution (larger file)
isolated contract contraction:
http://www.ncvs.org/ncvs/library/tech/note3/high/musc3d_contract.gif
elongate contract contraction:
http://www.ncvs.org/ncvs/library/tech/note3/high/musc3d_elong.gif

For completeness, Figure 1.9 shows the final composite of the posturing model with all boundary conditions marked as discussed in Hunter (2001) and Hunter et al. (2004).

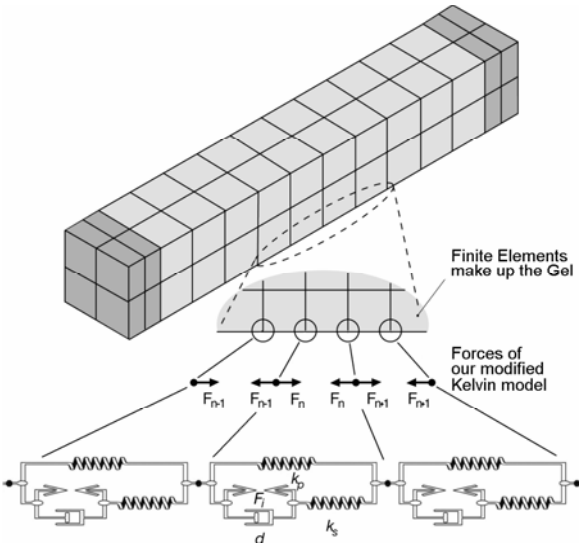

Figure 1.8. Model of an isolated muscle with cartilage on both ends (shaded) with forces from the modified Kelvin fiber model superimposed on specific nodes in series to add viscous losses and contraction forces.

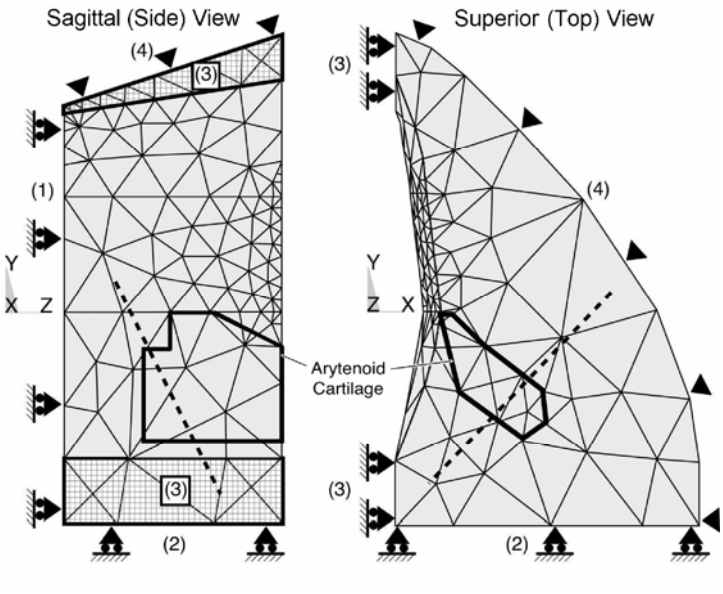

Figure 1.9 Three-dimensional vocal fold model divided into 1721 elements with only surface element faces shown. Four surface constraints within the model: (1) inferior (bottom) border, (2) posterior (back) border, (3) medial border, and (4) latero-anterior (thyroid cartilage) border. CAJ axis (dotted line) shown passing though the arytenoid cartilage (represented by the dark outline).

2. Dynamics of modeled vocal fold posturing

Using the Hunter model, each laryngeal muscle was contracted at 100-percent activity. From these contractions, the resulting deformations were recorded for visualization.

Muscle	*low resolution (small file)*	*high resolution (larger file)*
PCA	http://www.ncvs.org/ncvs/library/tech/note3/low/pca2.gif	http://www.ncvs.org/ncvs/library/tech/note3/high/pca2.gif
LCA	http://www.ncvs.org/ncvs/library/tech/note3/low/lca2.gif	http://www.ncvs.org/ncvs/library/tech/note3/high/lca2.gif
IA	http://www.ncvs.org/ncvs/library/tech/note3/low/ia2.gif	http://www.ncvs.org/ncvs/library/tech/note3/high/ia2.gif
TAM	http://www.ncvs.org/ncvs/library/tech/note3/low/tam2.gif	http://www.ncvs.org/ncvs/library/tech/note3/high/tam2.gif
TAV	http://www.ncvs.org/ncvs/library/tech/note3/low/tav2.gif	http://www.ncvs.org/ncvs/library/tech/note3/high/tav2.gif

Three landmarks on the model were tracked during each muscle contraction. The first two landmarks were near the vocal process (VPS and VPM, as defined below); the third landmarks showed the motion of the arytenoid's translation at the rocking-sliding axis (CAJ_P). The CAJ_P point was chosen because tracking the motion of this point would be useful to those researchers using the rocking-sliding construct. Although the exact position of the vocal process can be defined in the model, its actual location would be difficult to pinpoint in video endoscopic research. Thus, to account for potential variations, two possible positions were pinpointed to represent the vocal process (or the vocal fold edge near the vocal process). These positions were: 1) the point on the superior surface of the vocal folds directly above the actual vocal process, VPS (Figure 2.1, Point C); and 2) the most medial point (which changes with bulging) on the vocal fold's medial surface directly left of the actual vocal process, VPM (Figure 2.1, Point D). These points were approximately 0.7 mm apart, medio-laterally.

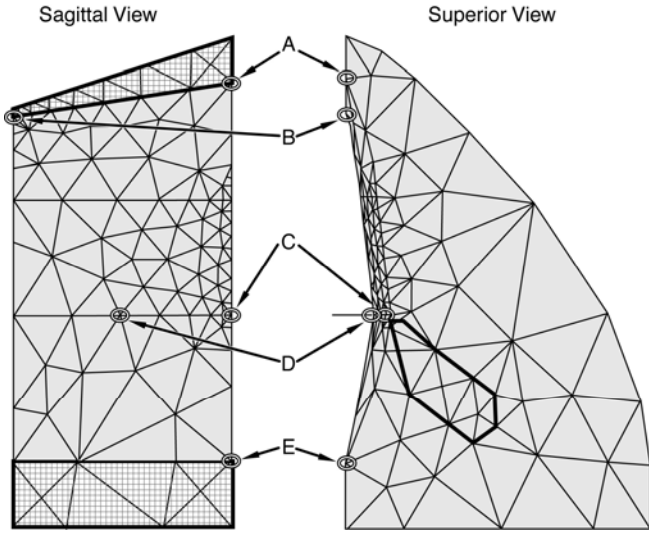

Figure 2.1. Landmark points on the model used to calculate glottal angle were chosen from the most likely points used to make glottal angle measurements in an endoscopic exam. Point A- model's superior anterior commissure used as the angle vertex. Point B- model's inferior anterior commissure used as another possible vertex. Point C- superior edge of vocal fold at the vocal process. Point D- most medial point directly inferior to Point C, which may vary superiorly and inferiorly depending on bulging. Point E- posterior glottis. The first unilateral glottal half angle is made using Points D-B-E with the next three made of D-A-E, C-B-E, and C-A-E respectively.

From VPS and VPM, three sets of measurements were determined: 1) absolute glottal width and absolute glottal width velocity (GW and dGW); 2) normalized glottal width (defined below) and normalized glottal width velocity (GWN and dGWN); and 3) glottal angle and glottal angle velocity (GA and dGA). Each of these measurements was calculated for both of the landmarks VPS and VPM independently. GWN was measured with respect to GW at a GA of 20 degrees (after Cooke et al., 1997). As only the right fold was modeled, the GA was defined as twice the angle between the midline (or posterior commisure, Figure 2.1, Point E) and the vocal process (both VPS and VPM), with the anterior commissure as the vertex (Figure 2.1, average of Points A and B). VPS, VPM, and CAJ_P were tracked during the dynamic deformations shown above caused by the muscle contractions (Figures 2.2-2.6). Figure 2.7 depicts GW, dGW, GWN, dGWN, GA, and dGA.

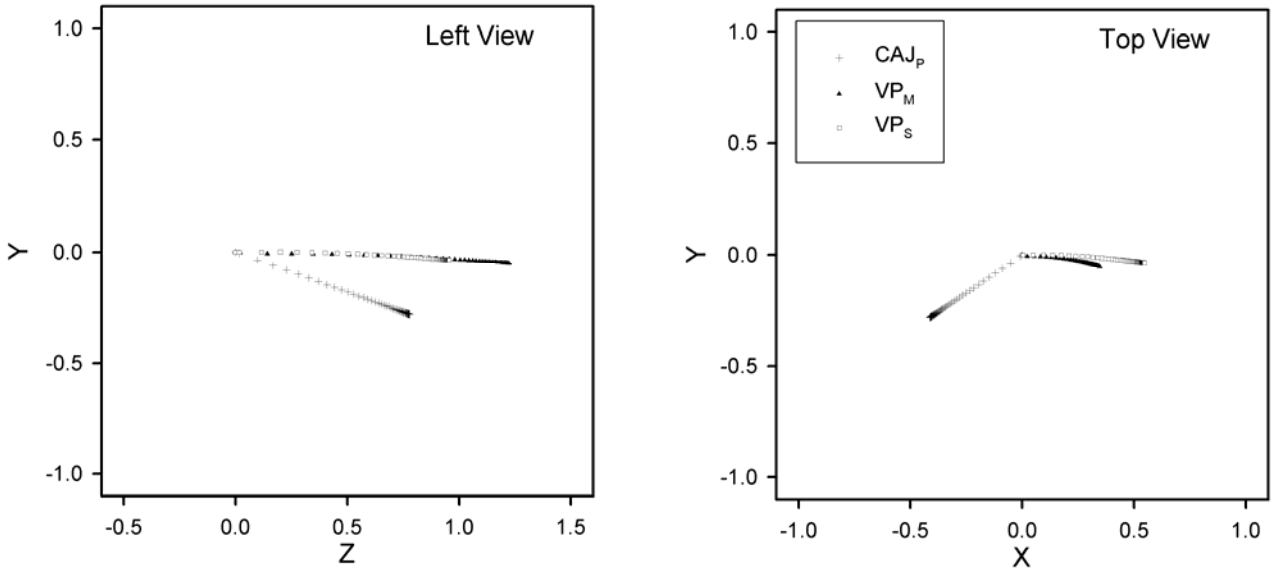

Figure 2.2. Top and side views of modeled displacement paths of the two possible vocal process positions and the CAJ_P joint location as a result of IA contraction.

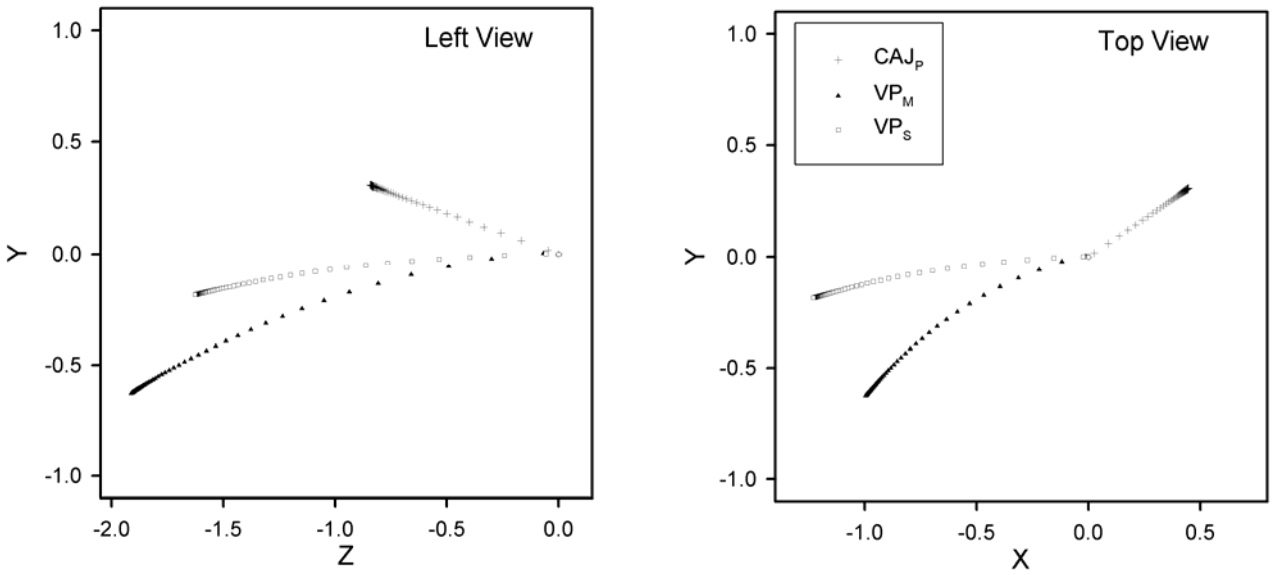

Figure 2.3. Top and side views of modeled displacement paths of the two possible vocal process positions and the CAJ_P joint location as a result of LCA contraction.

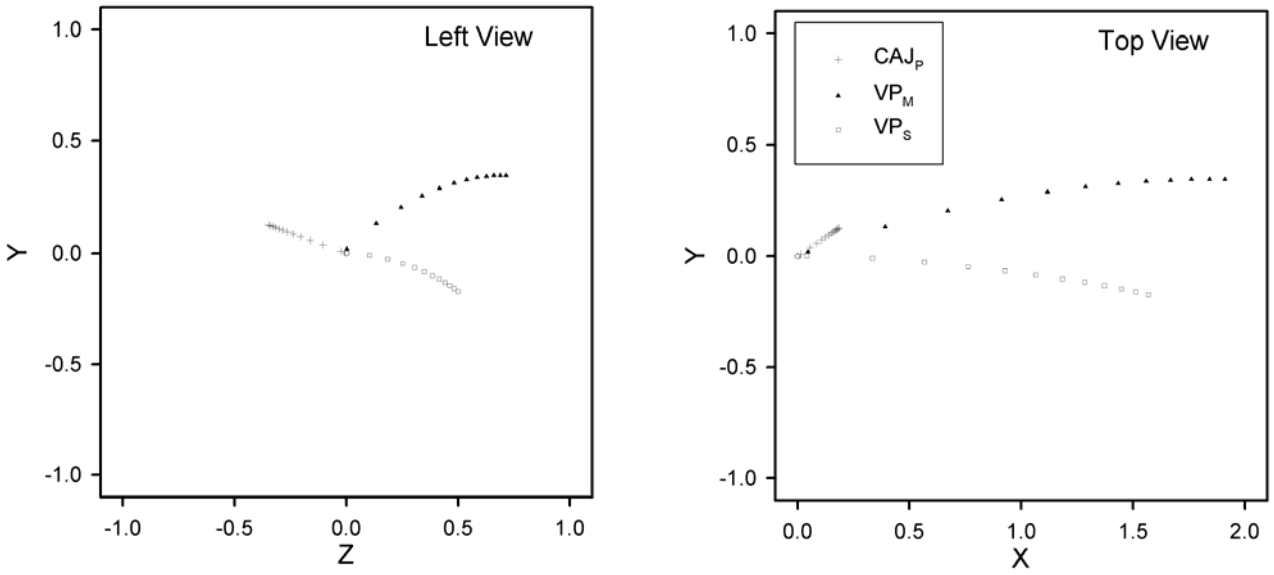

Figure 2.4. Top and side views of modeled displacement paths of the two possible vocal process positions and the CAJ_P joint location as a result of PCA contraction.

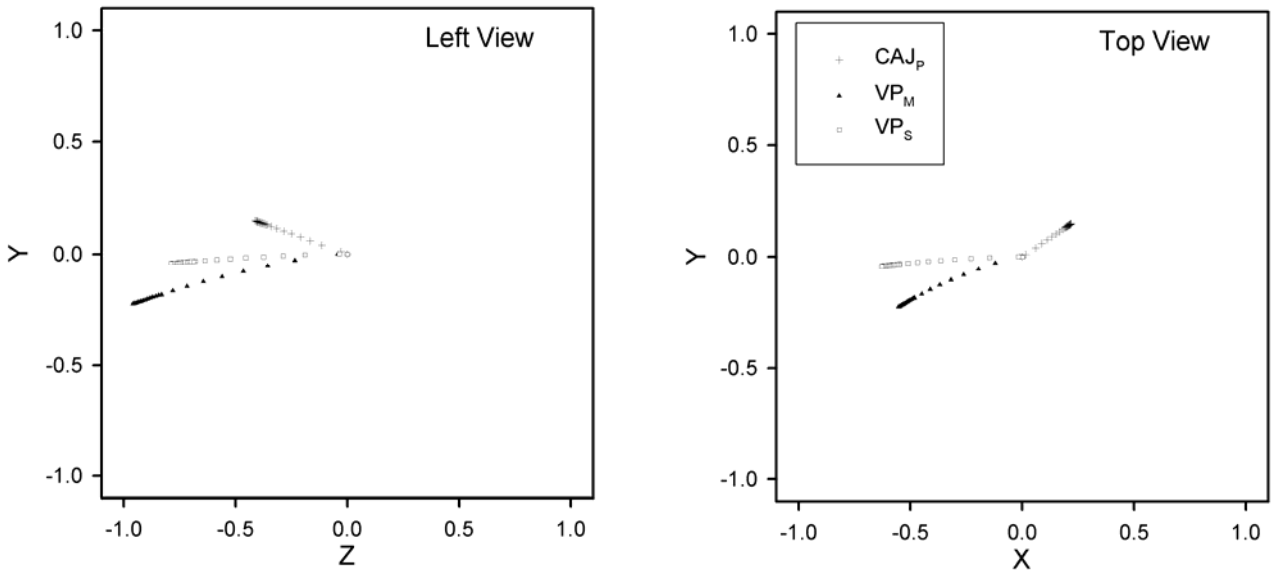

Figure 2.5. Top and side views of modeled displacement paths of the two possible vocal process positions and the CAJ_P joint location as a result of TAM contraction.

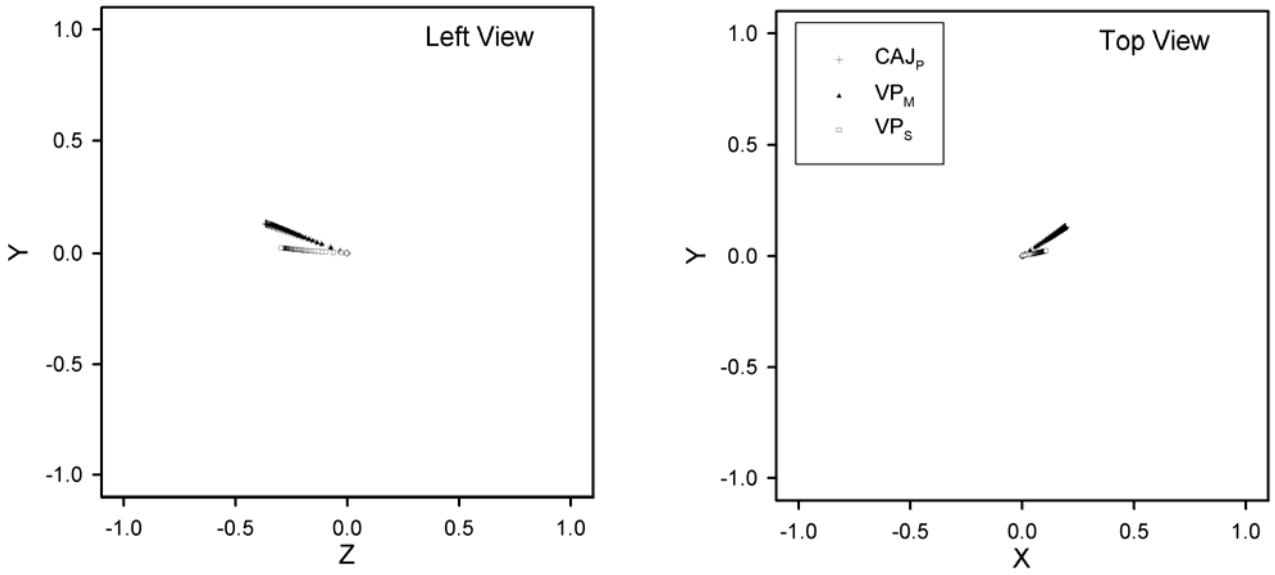

Figure 2.6. Top and side views of modeled displacement paths of the two possible vocal process positions and the CAJ_P joint location as a result of TAV contraction.

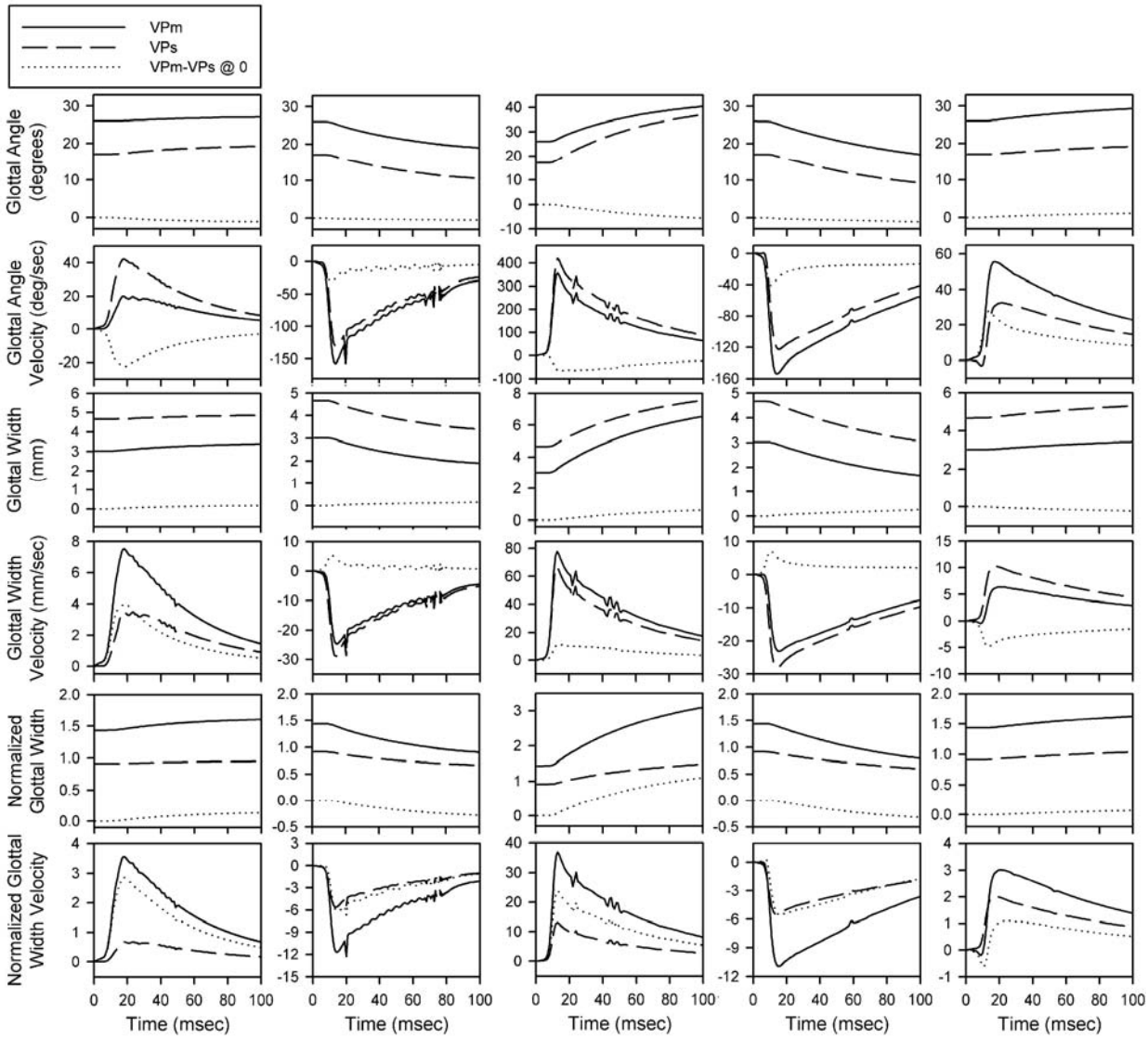

Figure 2.7. Modeled paths of glottal width (GW), normalized glottal width (GWN, after Cooke, et.al., 1997), glottal angle (GA) and their respective velocities (dGA) for each laryngeal muscle attached to the arytenoid cartilage. The two paths for each figure box represent two possible glottal vocal process positions if subjectively located. Dotted lines represent differences between the two vocal process position motions. Anomalies in some velocity contours are numerical artifacts from changes in sampling rate of model solution. (from left to right: IA, LCA, PCA, TAM, TAV contraction)

3. Muscle Scripts in APDL

The three-dimensional model of vocal fold abduction/adduction is a dynamic model where the individual muscles are both the generators of motion and stress (via contraction) as well as the primary responders to motion (via nonlinear passive stress-strain). Included in the passive nonlinear response is the vocal ligament, which can be thought of as a muscle without the ability to contract. The papers referenced above (Hunter, 2001; Hunter et al. 2004), gives the

time dependent differential equations describing passive and contractile axial stress in these tissues. Within Hunter et al., reference is made to special subroutines written in APDL to include the fiber contributions of the muscles. In this section the muscle equations from the paper are shown in terms of scripts written in APDL. No attempt is made in this memo to discuss the basic uses of ANSYS or APDL because it was assumed that the reader would have some basic knowledge of this. However, APDL does have some similarities to both FORTRAN and MATLAB scripts and, thus, the scripts included in this memo are likely to be understood by those with programming experience and can be translated into an analysis language of their choice. It is requested that any use of these scripts in any form or translation make reference to this memo. The current scripts have only been tested with ANSYS 5.7. They are directly available at http://www.ncvs.org/ncvs/library/tech .

http://www.ncvs.org/ncvs/library/tech/NCVSmemo03files.zip

kelvin_p.mac

This function represents the solution of the differential equations using a fourth order Runge-Kutte method for Equations 21 and 22 from Hunter et al. (2004). This function was based on FORTRAN code written by Ingo Titze in which the two-dimensional posturing of the arytenoid is calculated for a speech simulator. Conversion, translation and modifications from FORTRAN to APDL was made by Eric Hunter in 2001.

Description: This function calculates the stress to apply to a node for nonlinear (contractile and/or passive) material given time step, time, strain, strain history, and activation percentage. All other muscle constants from Kelvin Model must already be defined in memory.

Usage: Kelvin variables *tau*, *time*, *eps*, *deps*, *atv*, *sigT*, *dsigT*, *sigI*, and *dsigI* are respectively assigned to *arg1*, *arg2*, *arg3*, *arg4*, *arg5*, *arg6*, *arg7*, *arg8*, and *arg9* when calling the function. Upon completion, the function returns the variables: *SigI_* (internal stress), *SigT_* (total stress), *dSigI_* (internal stress), *dSigT_* (total stress), *E_* (tanjent youngs modulus), *Time1_* (time after runga-kutta), and *SigP_* (passive stress).

This function requires the following scripts to be previously executed: *jun23_MuscData.inp* and *musparam.mac*. This function also requires the following functions to be available: *active.mac*, *passive.mac*, *maximum.mac*, and *rkfor.mac*.

jun23_MuscData.inp

An input file contains muscle information for all the different muscles used in the model. This can be run without other initializations. All variables are self contained. The script returns three arrays that contain Kelvin Model parameters, direction cosines, cross-sectional area, and muscle length.

musparam.mac

This is a macro that assigns Kelvin Model parameter values and direction cosines from a specific tissue type. It requires that the muscle data be already present in memory (as assigned by 'jun23_MuscData.inp').

active.mac

This function calculates the active axial stress of a muscle. It represents Equation 18, 19, and 20 from Hunter et al. (2004)

Usage: equation variables *a*, *eps*, *sigm*, *bb*, *epm*, *depm*, *deps* are respectivly assigned on function call as *arg1*, *arg2*, *arg3*, *arg4*, *arg5*, *arg6*, *arg7* (see line 99 in *kelvin_p.mac*). Upon completion, the function returns the variable *tmp_*, the total predicted active axial stress in the muscle.

passive.mac

This function calculates the passive nonlinear axial stress within elongated tissue. It represents Equation 13 and 14 from Hunter et al. (2004).

Usage: equation variables *sg0*, *sg2*, *epsy*, *ep1*, *ep2*, *B*, are respectively assigned on function call as *arg1*, *arg2*, *arg3*, *arg4*, *arg5*, arg6 (see line 112 in *kelvin_p.mac*). Upon completion, the function returns the variable *tmp_*, the total predicted axial passive stress in the muscle.

maximum.mac

This is a generic APDL function that returns the maximum of two given variables.

rkfor.mac

This is a fourth order Runge-Kutte routine adapted from Ingo Titze's FORTRAN version.

All these files are packed together in the file *scripts.zip*.

Literature

Cox, K. A., Alipour, F., and Titze, I. R. (1999), “Geometric structure of the human and canine cricothyroid and thyroarytenoid muscles for biomechanical applications,” Ann. Otol. Rhinol. Laryngol. 108(12), 1151-8.

Hunter, E. J. (2001), Three-Dimensional Biomechanical Model of Vocal Fold Posturing. Ph.D. Dissertation. University of Iowa.

Hunter, E. J., Titze, I. R., and Alipour, F. (2004). “A three-dimensional model of vocal fold adduction/abduction,” J. Acoust. Soc. Am. (115)4, 1747-59.

Mineck, C. W., Tayama, N., Chan, R., and Titze, I. R. (2000), “Three-dimensional anatomic characterization of the canine laryngeal abductor and adductor musculature,” Ann. Otol. Rhinol. Laryngol. 109(5), 505-13.

Selbie, W. S., Zhang, L., Levine, W. S., and Ludlow, C. L. (1998). "Using joint geometry to determine the motion of the cricoarytenoid joint," J. Acoust. Soc. Am. (103)2, 1115-27.

Acknowledgements

This work was supported by NIDCD grant No DC04347-03 from National Institutes of Health. Thanks to the Denver Center for the Performing Arts and their continued support as the NCVS Denver site host. Thanks also to other members of our team at both Denver and the NCVS University of Iowa Site, namely Fari Alipour.

Copyright

Revisions

1.0 Eric Hunter: Main document (April 2004)
1.1 Eric Hunter: Minor edits, and clarifying text (Jan. 2005)